

1 **A comprehensive study of stable carbon and oxygen isotopes for *Cathaica***  
2 ***pulveratrix* and *Metodontia yantaiensis* land snails over last two glacial**  
3 **cycles at Beiyao site, central China: implications for paleovegetation and**  
4 **climate seasonality**

5

6 Ben Qin<sup>1,2</sup>, Xu Wang<sup>1,3,4</sup>, Yan Wu<sup>5</sup>, Shuisheng Du<sup>6</sup>, Linlin Cui<sup>1,4</sup>, Zhongli Ding<sup>1,3,4</sup>

7

8 *Author affiliation:*

9 1. Key Laboratory of Cenozoic and Environment, Institute of Geology and Geophysics,  
10 Chinese Academy of Sciences, P.O. Box 9825, Beijing 100029, China

11 2. China University of Geosciences (Beijing), Beijing, 100083, China

12 3. CAS Center for Excellence in Life and Paleoenvironment, Beijing, China

13 4. Innovation Academy for Earth Science, CAS

14 5. Anhui Museum, Hefei, 230081, China

15 6. School of History, Beijing Normal University, Beijing 100875, China

16 *Corresponding author:* Xu Wang

17 Phone: +86-10-82998581

18 Fax: +86-10-62010846

19 E-mail: [xuking@mail.iggcas.ac.cn](mailto:xuking@mail.iggcas.ac.cn)

20

21 **Key Points:**

- 22 •  $\delta^{18}\text{O}$  and  $\delta^{13}\text{C}$  of *C. pulveratrix* and *M. yantaiensis* snails over last 20 ka were studied  
23 to trace paleoclimate and paleovegetation changes.
- 24 •  $\delta^{18}\text{O}$  showed more rainfall during MIS3 and MIS7 stages and an overall 1.5 times  
25 stronger seasonality during glacial than interglacial period.
- 26 •  $\delta^{13}\text{C}$  revealed more  $\text{C}_4$  biomass during warm/humid MIS3 and MIS7 stages and *M.*  
27 *yantaiensis* ingested more  $\text{C}_4$  than *C. pulveratrix*.

28

29 **Abstract**

30 Modern investigations have shown that oxygen and carbon isotopes of land snail shells are  
31 useful indicators of climate and vegetation in monsoonal region. However, stable isotope  
32 study on snail fossil shells in strata has been seldom done, and the reliability of those  
33 indicators needs further verification. Moreover, intra-shell stable isotope analysis of  
34 individual snail is rather scarce, and seasonal variation of the glacial-interglacial monsoonal  
35 climate remains unclear. In this context, we performed  $\delta^{18}\text{O}$  and  $\delta^{13}\text{C}$  analyses on fossil  
36 shells of cold-aridiphilous *Cathaica pulveratrix* and sub-humidiphilous *Metodontia*  
37 *yantaiensis* from the loess section over the last two glacial cycles at Beiyao site in southern  
38 Chinese Loess Plateau. The  $\delta^{18}\text{O}$  of fossil shells reflected monsoonal rainfall amount and  
39 more rainfall during MIS3 and MIS7. Meanwhile, the  $\delta^{13}\text{C}$  of fossil shells indicated relative  
40 abundance of  $\text{C}_3/\text{C}_4$  plants and more  $\text{C}_4$  biomass during MIS3 and MIS7. The  $\delta^{18}\text{O}$  and  
41  $\delta^{13}\text{C}$  of the two species from the same horizon are significantly different, reflecting  
42 differences in their growing season and/or physiological habits. Intra-shell variations of stable  
43 isotopes showed that climatic seasonality was relatively strong during the glacial periods

44 whereas seasonality became weakened during the interglacials. Our findings provide an  
45 environmental background for explaining past human activities at the Beiyao site. The  
46 investigation of stone artifacts showed that ancient human activities were relatively strong  
47 during MIS3 and MIS7. During these stages, the warm and humid climate with smaller  
48 seasonal contrast was favorable for the regional expansion of human activities.

49

## 50 **1 Introduction**

51 Land snails are ideal materials for paleoclimate studies (Goodfriend, 1992; Wang et al.,  
52 2016; Wu et al., 2018). This is because they have advantages of being widely distributed,  
53 abundant and well preserved in strata. And they are relatively sensitive to climate changes. To  
54 date, researches on land snails include inferring the environmental conditions under which  
55 land snails survived through identifying faunal assemblage and living habit of each species  
56 (Gittenberger and Goodfriend., 1993; Wu et al., 2008), and reconstructing the paleoclimates  
57 through analyzing stable isotopes of land snail shells (Goodfriend and Ellis, 2002; Liu et al.,  
58 2006; Gu et al., 2009; Colonese et al., 2010; Rangarajan et al., 2013; Yanes and Fernández-  
59 Lopez-de-Pablo, 2016; Prendergast et al., 2016; Padgett et al., 2019).

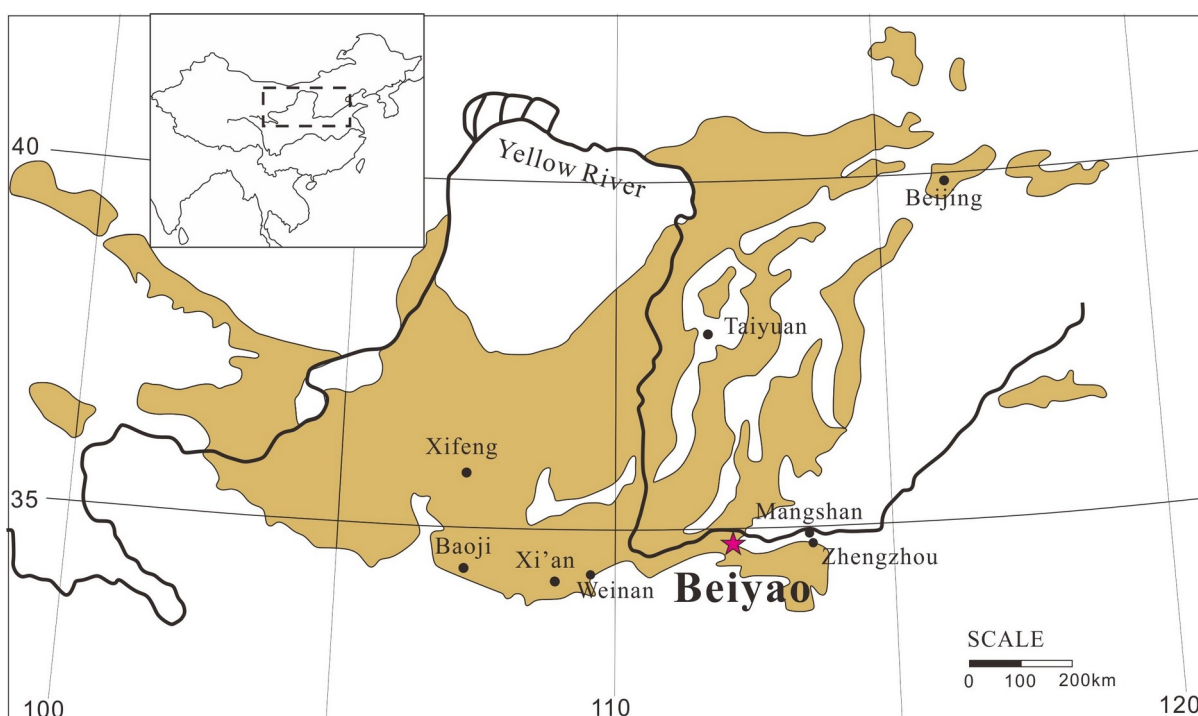
60 Theoretically, oxygen isotope in snail shell is determined by the oxygen isotope of snail  
61 body water and the temperature under which shell carbonate precipitates. Although body  
62 water oxygen isotopes of land snails are modified to different extents by evaporation due to  
63 differences in physiological habits of various species, it can still be generally used to track  
64 changes in precipitation oxygen isotopes (Zarrur et al., 2011; Zhai et al., 2019). Therefore, in  
65 the case of little temperature change, oxygen isotopes of land snail shells mainly reflect  
66 oxygen isotopes of rainfall (Prendergast et al., 2016; Wang et al., 2016; Milano et al., 2018;

67 Padgett et al., 2019). The snail shell carbon isotope reflects the carbon isotope composition of  
68 food they intake, with a large proportion of dietary plants, e.g., organic food accounts for  
69 more than 70% of carbon sources of land snail shell (Xu et al., 2010). In brief, the shell  
70 carbon isotope value can provide information on the relative abundance of C<sub>3</sub>/C<sub>4</sub> plants in the  
71 food(Goodfriend and Ellis, 2002; Prendergast et al., 2017).

72 Land snail fossils are abundant and widely distributed in the Asian monsoon region,  
73 especially in the Chinese Loess Plateau (Wu et al., 1996 ; Wu et al., 2002; Liu et al., 2006;  
74 Gu et al., 2009). However, researches on the stable isotopes of snail shells have mainly  
75 focused on studying modern land snails in different climatic regions (Liu et al., 2006; Wang  
76 et al., 2016; Bao et al., 2018, 2019; Wang et al., 2019; Zhai et al., 2019). In contrast, stable  
77 isotope analyses of fossil snails in strata have been inadequently done, and only a few species  
78 of land snails were studied (Gu et al., 2009; Huang et al., 2012). In this context, it is  
79 necessary to perform stable isotope analyses on shell fossils of different land snail species  
80 from strata in the different regions and compare those data with other paleoclimatic proxy  
81 indicators to confirm their paleoenvironment and paleoclimate significances. Moreover,  
82 stable isotope analysis of individual shell along shell ontogeny has the potential to provide  
83 seasonal information (Leng et al., 1998; Goodfriend and Ellis, 2002). However, the  
84 application of this type of research in paleoclimate is also less developed.

85 In this study, we systematically collected land snail fossils from loess-paleosol section over  
86 last two glacial-interglacial cycles at the Beiyao site in Luoyang, central China. Carbon and  
87 oxygen isotopes were measured on *Cathaica pulveratrix* (cold-aridiphilous) and *Metodontia*  
88 *yantaiensis* (sub-humidiphilous) land snails. We then compared these isotopic data with  
89 paleoclimate proxy indicators like grain size and magnetic susceptibility with attempt to  
90 reconstruct changes in climate and vegetation (C<sub>3</sub>/C<sub>4</sub> plants) in the study area. The Luoyang

91 Beiyao site is an archaeological site with human activities in the Paleolithic Age. Recent  
92 studies have found some lithics in strata belonging to the late glacial period and the middle  
93 and late MIS7 stage (Du et al., 2011; Du and Liu, 2014), indicating that there were human  
94 activities during those time periods. However, the climate and environmental context  
95 associated with the human activities is still unclear. This study will precisely analyze the  
96 environmental conditions for the human activities during the late glacial period and the  
97 middle and late of MIS7. At the same time, we also selected snail fossils during the typical  
98 periods of the glacials and interglacials, and analyzed intra-shell isotopic variation of each  
99 shell to obtain seasonal information during these periods, thereby helping us to understand  
100 changes in climatic seasonality from glacial to interglacial period.



101  
102 **Figure 1.** Location map of the study site (red star). The yellow shaded area is the distribution  
103 range of the Loess Plateau, edited from Kukla and An (1989).

104

## 105 **2 Geological settings and sample collection**

### 106 2.1 Geological settings

107         The loess-paleosol section is located at the Luoyang Beiyao archaeological  
108 site (  $34^{\circ}42'24''\text{N}$  ,  $112^{\circ}28'46''\text{E}$  ) on the southeast edge of the Chinese Loess Plateau  
109 (Figure 1). The Beiyao site lies on the third-grade loess accumulation terrace on the south  
110 bank of the Luo River in Luoyang. The terrace is about 20m higher than the modern river  
111 bed, and the loess section is 16.7m long from bottom to top. Grain size and magnetic  
112 susceptibility data combined with optical luminescence (OSL) and AMS  $^{14}\text{C}$  datings showed  
113 that the loess section has covered the last two glacial-interglacial cycles (Du et al., 2011). At  
114 present, the mean annual temperature and annual precipitation are  $14.2^{\circ}\text{C}$  and 546 mm,  
115 respectively. The study area is located in a typical monsoonal region. Northerly wind prevails  
116 and climate is cold and dry in winter, while southerly wind dominates in summer with hot  
117 and rainy condition. A large number of stone artifacts were found in the Beiyao section at  
118 depth of 6.5~7.5m and 11~13m, indicating that there were prehistoric human activities.

119         The magnetic susceptibility and median particle size curves showed synchronous changes,  
120 and had a good correspondence with the marine oxygen-isotope stage (MIS) curve (Tang et  
121 al., 2017). Therefore, in this study, we sub-divided the loess section to various oxygen isotope  
122 stages according to the grain size and magnetic susceptibility, referring to AMS  $^{14}\text{C}$  and OSL  
123 datings.

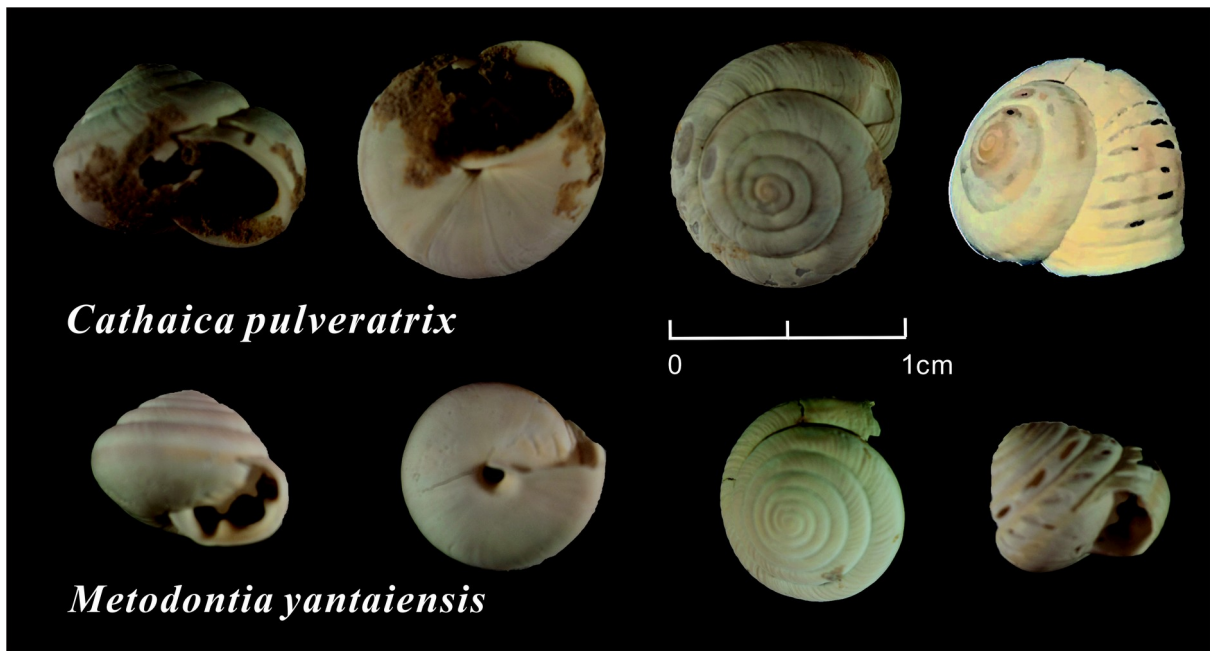
### 124 2.2 Collection of land snail fossils

125         During the sampling process at the Beiyao site,  $1\text{m} \times 1\text{m} \times 10\text{cm}$  volume loess (or  
126 paleosol) was continuously excavated downward, and the snails in each horizon were

127 collected by screening and washing using water and a 0.5 mm sieve. The identification and  
128 statistics of the snail fossils used in this study were completed by Yan Wu. Throughout the  
129 section, there were 1911 cold-aridiphilous *Cathaica pulveratrix* (*C. pulveratrix*) and 241 sub-  
130 humidiphilous *Metodontia yantaiensis* (*M. yantaiensis*) (Wu, 2011). When the fossil  
131 fragments were counted as Quaternary loess snail individuals, the calculation method  
132 developed by Puisségur (1976) was used to convert the fragments into snail fossil individuals  
133 and sum them as the total number of individuals. The conversion formula (Puisségur, 1976)  
134 is as followed:

$$\text{Number of individuals} = \frac{\text{number of fragments}}{5} - \frac{\text{number of fragments}}{5} \times \text{conversion factor}$$

137 The conversion factor varies with the number of snail fossil fragments. When the number  
138 of snail fossil fragments is <50, 50-75, 75-100, and >100, the conversion factor is 10%, 20%,  
139 33%, and 50%, respectively. Except for few fossils due to the strong pedogenesis at 6.8-7m,  
140 most of the section is rich in snail fossils. In this study, we used complete shell of land snails  
141 for stable isotope analysis. Totally, there are 577 *C. pulveratrix* shells from 59 horizons, and  
142 97 *M. yantaiensis* shells from 15 horizons.



143

144 **Figure 2.** Photos showing shell morphology of the two species land snails. The sampling  
 145 strategy along with the growth band was also shown.

146

147 2.3 Ecological habits of the two species

148 The two species of land snails used in this study have different living habits. *C. pulveratrix*  
 149 usually lives in relatively cold and dry climates whereas *M. yantaiensis* lives in warm and  
 150 sub-humid climates (Wu et al., 1996; Chen and Wu, 2008). The pictures for two species of  
 151 land snails are shown in Figure 2. Both species are also living in the modern time. According  
 152 to Chen (2016), *C. pulveratrix* distributes over a vast area including Shanxi, Henan, Hunan,  
 153 Shaanxi, Gansu, Xinjiang provinces, and even in central Asia. The habitat for *C. pulveratrix*  
 154 is usually in thick grasses or under the litter beneath trees in mountain area, on flat slope of  
 155 hills as well as in ranches, orchards and crop land. *M. yantaiensis* distributes usually in  
 156 northern China, i.e., Beijing, Tianjin, Hebei, Shanxi, Inner Mongolia, Shandong and Shaanxi,  
 157 and also shows in area around the Yangtze River. It often lives in slightly damp bushes,  
 158 grasses, under rocks and leaves in in mountainous and hilly areas.

159 Shell size comparison shows that *C. pulveratrix* is usually larger than *M. yantaiensis* (Table  
 160 1). This morphology difference complies with their living environment conditions. According  
 161 to previous studies, the large shell can reduce the ratio of surface area to volume, thereby  
 162 limiting water evaporation and making it easier for the snails to survive in drier  
 163 environments ( Nevo et al., 1983; Yanes and Fernández-Lopez-de-Pablo, 2016 ) .

164

165 **Table 1** Snail shell sizes of the two species at various MIS stages.

| Genus                | MIS3                  |                       | MIS4                  |                       | MIS6                  |                       | MIS7                  |                       |
|----------------------|-----------------------|-----------------------|-----------------------|-----------------------|-----------------------|-----------------------|-----------------------|-----------------------|
|                      | <i>M. yantaiensis</i> | <i>C. pulveratrix</i> |
| Spiral ( number )    | 5                     | 5                     | 5                     | 5                     | 7                     | 5                     | 6                     | 5                     |
| Height ( cm )        | 0.55                  | 1.5                   | 0.5                   | 1.2                   | 0.95                  | 1.3                   | 0.8                   | 1.1                   |
| Height of lip ( cm ) | 0.3                   | 0.85                  | 0.3                   | 0.7                   | 0.4                   | 0.7                   | 0.4                   | 0.7                   |
| Width of lip ( cm )  | 0.35                  | 0.7                   | 0.35                  | 0.6                   | 0.5                   | 0.7                   | 0.5                   | 0.8                   |

166

### 167 **3 Materials and Methods**

#### 168 3.1 Snail shells pretreatment and sampling strategy

169 The entire shell was firstly cleaned with distilled water, and the soil particles attached to  
 170 the shell surface were brushed using a toothbrush, and then the shell was placed in a drying  
 171 oven and heated at 60 °C for 12 hours. The relatively large shells were chosen for sampling  
 172 along the growth band. Firstly, we removed the residual clay cements on the surface of shells  
 173 using a dental drill, then cleaned the shells using a ultrasonic utility for multiple times, and

174 finally dried the shells in an oven. The three dimension of each shell (i.e.,shell height, width  
175 and height of shell mouth) was measured using a ruler. For intra-shell sampling, we use a  
176 micro drill to take powders from the shell lip till apex at 1-2 mm interval along the growth  
177 direction of the snail (Figure 2). The drill bit was soaked in diluted hydrochloric acid solution  
178 after each sample to remove residual carbonate powder on it.

179 For the carbon and oxygen isotope analyses of the whole shell, about 10 shells were  
180 combined according to the availability of snail shells in each horizon. This can ensure the  
181 measured data to represent a general and average environment condition under which land  
182 snails lived. After the shell was cleaned and dried for the first time, it was broken into  
183 fragments. The clay cement attached to each shell fragment was physically removed, and then  
184 the fragments were further cleaned using an ultrasonic utility. After very clean shell  
185 fragments were obtained, we dried them in an oven at 60 °C. Finally, we ground them into  
186 powders and homogenized using a mortar and pestle.

### 187 3.2 Stable isotope analyses

188 The carbon and oxygen isotopic analyses of the snail shell powder were performed on the  
189 GasBench II multifunctional gas preparation system coupled with the Delta V Plus isotope  
190 ratio mass spectrometer (Thermo Fisher). A 100µg carbonate powder reacted with 100%  
191 H<sub>3</sub>PO<sub>4</sub> at 72 °C for 1 hour. The generated CO<sub>2</sub> passed through two NAFION™ water traps  
192 to remove trace water and passed through a PoraPlot Q chromatography column at 45 °C to  
193 separate with other impurities. After that, the CO<sub>2</sub> was introduced into the isotope ratio mass  
194 spectrometer to measure the carbon and oxygen isotope ratios. Both carbon and oxygen  
195 isotope data are reported relative to the VPDB. The standards used for data correction and  
196 calibration were GBW4416 ( $\delta^{13}\text{C}_{\text{VPDB}}=1.61\text{‰}$ ,  $\delta^{18}\text{O}_{\text{VPDB}}=-11.59\text{‰}$ ) and NBS19  
197 ( $\delta^{13}\text{C}_{\text{VPDB}}=1.95\text{‰}$ ,  $\delta^{18}\text{O}_{\text{VPDB}}=-2.20\text{‰}$ ). The analytical precision of carbon and oxygen

198 isotopes is 0.06‰ and 0.10‰, respectively. Detailed analytical method can be found in  
199 Wang et al. (2019).

## 200 4 Results

### 201 4.1 Carbon and oxygen isotopes of whole shell for two species land snails

202 The variation range of  $\delta^{18}\text{O}_{\text{VPDB}}$  for cold-aridiphilous *C. pulveratrix* was -2.16‰ to -  
203 8.13‰, and the average value was -5.03‰. The maximum value of  $\delta^{18}\text{O}_{\text{VPDB}}$  was at the  
204 depth of 1.1 m in the profile, which corresponds to MIS2, while the minimum value of  
205  $\delta^{18}\text{O}_{\text{VPDB}}$  was at the depth of 11.7m, which belongs to MIS7. The  $\delta^{18}\text{O}_{\text{VPDB}}$  value for sub-  
206 humidiphilous *M. yantaiensis* ranged from -7.34‰ to -9.71‰, with an average of -8.43‰.  
207 The maximum  $\delta^{18}\text{O}_{\text{VPDB}}$  value was at 4.6 m (MIS4) and the minimum at 11.6 m (MIS7).

208 The  $\delta^{13}\text{C}_{\text{VPDB}}$  for *C. pulveratrix* ranged from -3.17‰ to -6.62‰ with an average of -  
209 4.81‰. The maximum  $\delta^{13}\text{C}$  was at the depth of 10.1 m in the profile, which belongs to  
210 MIS6 whereas the minimum  $\delta^{13}\text{C}$  was at 6.6m, which corresponds to the MIS5. The range of  
211  $\delta^{13}\text{C}_{\text{VPDB}}$  for *M. yantaiensis* was between -3.05‰ and -5.03‰, and the average value was -  
212 3.95‰. The maximum  $\delta^{13}\text{C}_{\text{VPDB}}$  for *M. yantaiensis* showed at 3.4 m (MIS3) whereas the  
213 minimum  $\delta^{13}\text{C}_{\text{VPDB}}$  occurred at 12 m (MIS7).

### 214 4.2 Carbon and oxygen isotope changes along the growth band of individual shell

215 In the MIS3 and MIS5, intra-shell  $\delta^{18}\text{O}_{\text{VPDB}}$  variation for *C. pulveratrix* was from -12.3‰  
216 to 0.2‰, and the variation of  $\delta^{13}\text{C}_{\text{VPDB}}$  was between -6.9‰ and -4.9‰. In contrast, of the  
217 intra-shell variation of  $\delta^{18}\text{O}_{\text{VPDB}}$  for *M. yantaiensis* was relatively small, i.e., from -10.1‰ to  
218 -5.9‰. The intra-shell  $\delta^{13}\text{C}_{\text{VPDB}}$  ranged from -7.7‰ to -4.8‰ (Table 1).

219 During the MIS4 and MIS6 stages, the intra-shell  $\delta^{18}\text{O}_{\text{VPDB}}$  and  $\delta^{13}\text{C}_{\text{VPDB}}$  for *C. pulveratrix*

220 varied from -12.0‰ to -3.5‰ and from -7.8‰ to -2.6‰, respectively. The corresponding  
 221 intra-shell variations for *M. yantaiensis* were much larger, i.e., from -13.3‰ to -1.7‰ for  
 222  $\delta^{18}\text{O}_{\text{VPDB}}$  and from -11.7 to -0.6‰ for  $\delta^{13}\text{C}_{\text{VPDB}}$  (Table 1).

223 The cold-aridiphilous *C. pulveratrix* had a shell height of 1.1 to 1.5 cm, a shell lip height of  
 224 0.7 to 0.85 cm, and a shell lip width of 0.6 to 0.8 cm. In contrast, the sub-humidiphilous *M.*  
 225 *yantaiensis* had shell height ranging from 0.55 to 0.95 cm, shell lip height ranging from 0.3 to  
 226 0.4 cm, and shell lip width ranging from 0.35 to 0.5 cm (Table 2). Obviously, the shell of *C.*  
 227 *pulveratrix* was significantly larger than that of *M. yantaiensis*. As a result, the intra-shell  
 228 sampling number for *C. pulveratrix* was larger than that for *M. yantaiensis*.

229

230 **Table 2** Statistics for Intra-shell  $\delta^{18}\text{O}$  and  $\delta^{13}\text{C}$  variations of two species at various MIS  
 231 stages.

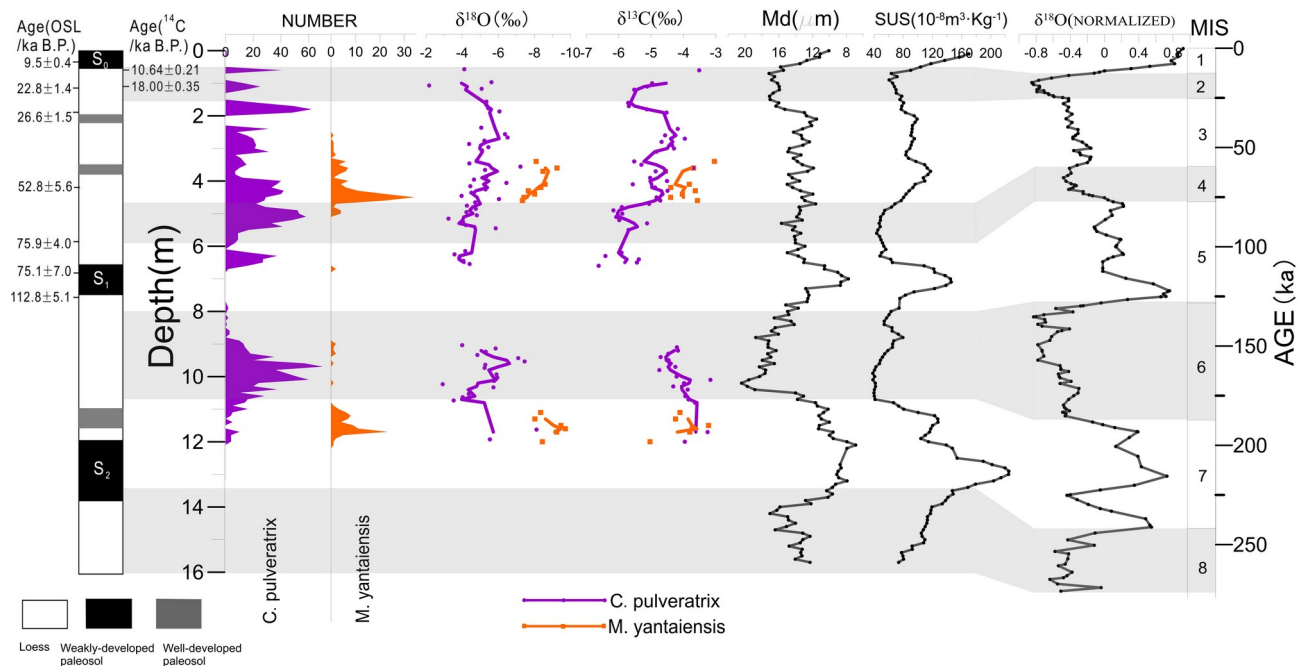
| Species               | Depth<br>( m ) | MIS | Number<br>of<br>sampling | $\delta^{18}\text{O}\%$<br>Average<br>( VPDB<br>) | $\delta^{18}\text{O}$<br>‰<br>Max | $\delta^{18}\text{O}\%$<br>Min | $\delta^{13}\text{C}\%$<br>Average<br>(VPDB) | $\delta^{13}\text{C}\%$<br>Max | $\delta^{13}\text{C}\%$<br>Min |
|-----------------------|----------------|-----|--------------------------|---------------------------------------------------|-----------------------------------|--------------------------------|----------------------------------------------|--------------------------------|--------------------------------|
| <i>C. pulveratrix</i> | 3.4            | 3   | 37                       | -9.5                                              | -6.4                              | -12.3                          | -5.6                                         | -4.9                           | -6.5                           |
| <i>C. pulveratrix</i> | 4.9            | 4   | 44                       | -4.7                                              | 0.3                               | -9.7                           | -4.7                                         | -2.6                           | -6.5                           |
| <i>C. pulveratrix</i> | 9.0            | 6   | 45                       | -3.6                                              | 3.5                               | -12.0                          | -5.2                                         | -4.1                           | -7.8                           |
| <i>C. pulveratrix</i> | 11.8           | 7   | 28                       | -5.7                                              | -0.2                              | -10.9                          | -6.2                                         | -5.1                           | -6.9                           |
| <i>M. yantaiensis</i> | 3.4            | 3   | 12                       | -9.8                                              | -8.7                              | -11.6                          | -6.4                                         | -5.1                           | -7.7                           |
| <i>M. yantaiensis</i> | 4.9            | 4   | 12                       | -10.5                                             | -7.8                              | -12.7                          | -1.6                                         | -0.6                           | -3.5                           |
| <i>M. yantaiensis</i> | 9.0            | 6   | 30                       | -5.7                                              | -1.7                              | -13.3                          | -10.4                                        | -8.7                           | -11.7                          |
| <i>M. yantaiensis</i> | 11.8           | 7   | 31                       | -10.1                                             | -5.9                              | -13.8                          | -6.2                                         | -4.8                           | -7.4                           |

232

### 233 4.3 Statistics of *C. pulveratrix* and *M. yantaiensis* in loess-paleosol strata

234 In the Beiyao section, the maximum number of cold-aridiphilous snails *C. pulveratrix* was  
 235 70, occurring at the depth of 9.7 m (belonging to MIS6). In contrast, the maximum number of

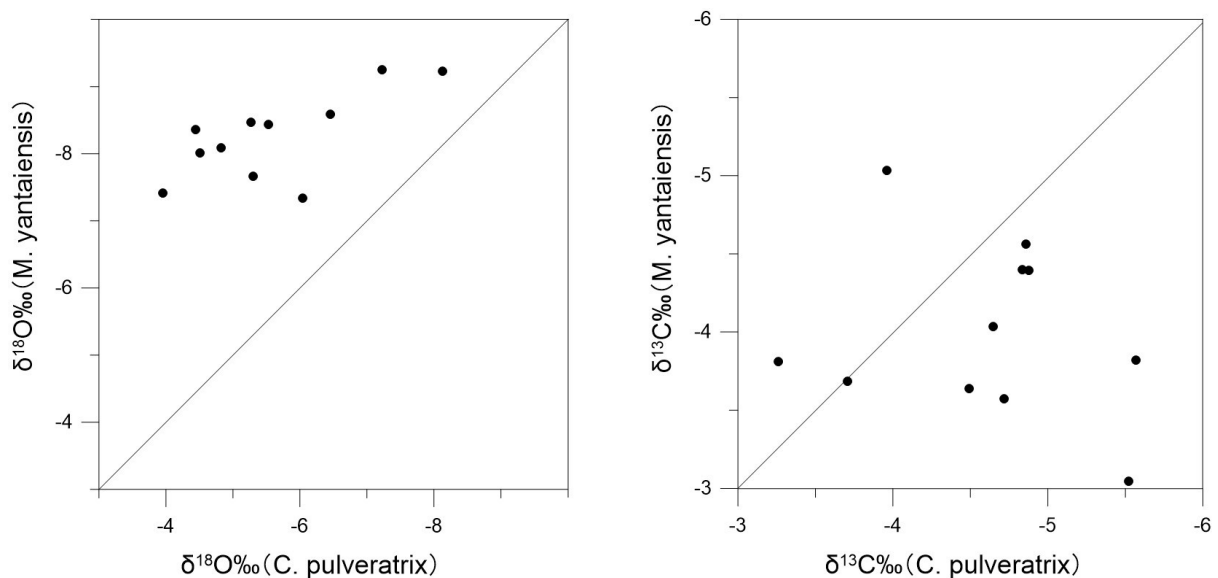
236 sub-humidiphilous snails *M. yantaiensis* was 34, appearing at the depth of 4.5 m (belonging  
 237 to MIS3) (Figure 3). At the bottom of the interglacial paleosol S1, very few of land snail  
 238 fossils were left because of the influence of strong pedogenesis. However, the other horizons  
 239 in the section were rich in snail fossils. Therefore, without considering this factor, the cold-  
 240 aridiphilous species *C. pulveratrix* had a certain number distributing from MIS2 to MIS7,  
 241 with two most abundant horizons (with fossil number of 58 and 70) respectively in MIS4 and  
 242 MIS6. The sub-humidiphilous species *M. yantaiensis* were mainly found in MIS3 and MIS7,  
 243 with maximum number reaching up to 34 and 23, respectively. Moreover, when the number  
 244 of *M. yantaiensis* increased in some horizon, the number of *C. pulveratrix* in the same  
 245 horizon or neighbouring horizons significantly reduced. Conversely, when the number of *C.*  
 246 *pulveratrix* reached the peak of the stage, the number of *M. yantaiensis* approached the  
 247 minimum or 0.



248

249 **Figure 3.** Changes in carbon and oxygen isotopes of *C. pulveratrix* and *M. yantaiensis* snails  
 250 over the last two glacial-interglacial cycles, in comparison with median grain size (Md),

251 magnetic susceptibility (SUS) and deep-sea  $\delta^{18}\text{O}$  curve. Stages partition, age data and  $\delta^{18}\text{O}$   
252 value(standardized) of MIS were from Martinson (1987), Md data were from Tang et al.  
253 (2017), SUS data were from Du and Liu (2014),  $^{14}\text{C}$  and OSL age data were from Du et al.  
254 (2011).



255  
256 **Figure 4.** Comparison of carbon and oxygen isotopes between *C. pulveratrix* and *M.*  
257 *yantaiensis* from the same horizon. Note that the  $\delta^{18}\text{O}$  value of *M. yantaiensis* was  
258 significantly lower than that of *C. pulveratrix*, while the  $\delta^{13}\text{C}$  value of *M. yantaiensis*  
259 was mostly higher than that of *C. pulveratrix*.

260

## 261 5 Discussion

### 262 5.1 Oxygen isotopes in land snail shells and changes in summer monsoon rainfall

263 Many studies have shown that oxygen isotope in land snail shell carbonate is positively  
264 related to oxygen isotope in atmospheric precipitation. (Gu et al., 2009; Prendergast et al.,  
265 2016; Wang et al., 2016; Milano et al., 2018; Padgett et al., 2019; Wang et al., 2019; Zhai et  
266 al., 2019). Generally speaking, the  $\delta^{18}\text{O}$  values of *C. pulveratrix* were more positive than

267 those of *M. yantaiensis* (Figure 4a). This is consistent with the eco-physiological habits of the  
268 two land snail species. The *M. yantaiensis* snails like to live in a relatively warm and humid  
269 environment and in seasons with more abundant rainfall. Due to the rainfall effect, the  
270 summer rainfall  $\delta^{18}\text{O}$  will be more negative, so  $\delta^{18}\text{O}$  in shell carbonate of *M. yantaiensis* is  
271 also relatively low. In contrast, the active season of *C. pulveratrix* is relatively cool and dry  
272 with less rainfall (such as spring and autumn), so relatively more positive oxygen isotope of  
273 rainfall during this time can result in relatively high  $\delta^{18}\text{O}$  in shell carbonate of *C. pulveratrix*.

274 Snail shell  $\delta^{18}\text{O}$  can be combined with other paleoclimate indicators such as the median  
275 grain size (Md), magnetic susceptibility (SUS) of the loess and faunal assemblages of land  
276 snails to indicate the strength of the East Asian summer monsoon (Wu et al., 2018). A  
277 previous study has shown that the shell  $\delta^{18}\text{O}$  of *C. pulveratrix* can be used as an indicator of  
278 summer precipitation to reflect the strength of the summer monsoon (Gu et al., 2009).  
279 Specifically, the shell  $\delta^{18}\text{O}$  of *C. pulveratrix* in the monsoon region of China decreased when  
280 the summer precipitation increased. This is consistent with the  $\delta^{18}\text{O}$  record of stalagmites in  
281 Hulu cave in Southern China (Wang et al., 2008).

282 Generally, the shell  $\delta^{18}\text{O}$  of *C. pulveratrix* showed a negative correlation with SUS and a  
283 positive correlation with Md in the Beiyao loess-paleosol section (Figure 3). This is  
284 consistent with the results of Gu et al. (2009). In the middle part of MIS7, the  $\delta^{18}\text{O}$  of *C.*  
285 *pulveratrix* exhibited a negative shift, with the minimum value being -8.13‰. Meanwhile,  
286 the Md value decreased, the number of cold-aridiphilous species *C. pulveratrix* decreased,  
287 and the number of sub-humidiphilous species *M. yantaiensis* increased (Figure 3). It  
288 suggested that the East Asian summer monsoon intensified during this period, and the  $\delta^{18}\text{O}$  of  
289 precipitation became more negative due to large amount of precipitation.

290 At the beginning of MIS6, the  $\delta^{18}\text{O}$  value of *C. pulveratrix* experienced a positive shift,

291 while the SUS value also became lower, indicating that the climate tended to be drier.  
292 Subsequently, the  $\delta^{18}\text{O}$  of *C. pulveratrix* showed a change to more negative value, with the  
293 most negative value reaching  $-7.5\text{‰}$ , and the Md value also became lower, indicating that  
294 there have been a significant increase in rainfall amount during the middle part of MIS6.

295 At the end of MIS5 and during MIS4, the  $\delta^{18}\text{O}$  values of *C. pulveratrix* snails were  
296 generally more positive, with an average  $\delta^{18}\text{O}_{\text{VPDB}}$  value of  $-4.2\text{‰}$ . At the same time, the  
297 SUS increased and the Md decreased. Collectively, it indicated a relative cold and dry  
298 climatic condition.

299 From MIS4 to MIS3, the  $\delta^{18}\text{O}$  of *C. pulveratrix* snail showed a significant decrease,  
300 indicating that the climate has entered a humid and rainy mode. However, the oxygen isotope  
301 became more positive during middle MIS3, which corresponded to the decrease in SUS. This  
302 implied that the climate during MIS3 was variable and there was once a relatively cold and  
303 dry climate. Despite this, the  $\delta^{18}\text{O}$  of *C. pulveratrix* during the middle MIS3 was still more  
304 negative than that during MIS4, indicating a slightly drying middle MIS3. The  $\delta^{18}\text{O}$  values of  
305 *C. pulveratrix* during the late stage of MIS3 were  $-0.6\text{‰}$  by average more negative than  
306 those during the early stage of MIS3, suggested a generally more humid climate during the  
307 late MIS3. But we acknowledged that the  $\delta^{18}\text{O}$  during the early MIS3 was highly variable  
308 and some negative extrema that are even lower than the late MIS3  $\delta^{18}\text{O}$  also appeared during  
309 this period. This may reflect some transient stages with much humid condition also occurred  
310 during the early MIS3. The three-stage sub-division of MIS3 can be also envisaged on the  
311 SUS curve of our loess section (Figure 3). The average  $\delta^{18}\text{O}$  value of *C. pulveratrix* was -  
312  $5.3\text{‰}$  during MIS3 stage. In contrast, the average  $\delta^{18}\text{O}$  during MIS2 was much higher (-  
313  $4.2\text{‰}$ ) and it showed a clear trend of increase, suggestive of a climatic transition from  
314 wetness to dryness.

315 Within MIS2 stage, the  $\delta^{18}\text{O}$  values of *C. pulveratrix* increased up to  $-2\text{‰}$  at about 21.6  
316 ka, which marked extreme dryness during the last glacial period (LGM). Similarly, the  $\delta^{18}\text{O}$   
317 of *C. pulveratrix* from Mangshan loess section in central China also showed an extremely  
318 positive value (approximately  $-1\text{‰}$ ) around 22 ka (Gu et al. 2009). The two study sites are  
319 about 100 km away. Collectively, it manifested a synchronous regional drought in central  
320 China during the LGM.

321 The  $\delta^{18}\text{O}$  values of *M. yantaiensis* exhibited almost the same pattern of variation as those  
322 of *C. pulveratrix* did. During late MIS7 stage, the  $\delta^{18}\text{O}$  of *M. yantaiensis* was more negative  
323 than that of *C. pulveratrix* and attained to the most negative of  $-9.71\text{‰}$  when the  $\delta^{18}\text{O}$  of *C.*  
324 *pulveratrix* dropped to its most negative one (Figure 3). In the meantime, SUS also increased  
325 its peak value. These lines of evidences corroborated abundant rainfall brought by the  
326 intensified summer monsoon during the late MIS7. During the early MIS3, the  $\delta^{18}\text{O}$  of *M.*  
327 *yantaiensis* showed a gradually decreasing trend, which was synchronous with the changes in  
328 *C. pulveratrix*  $\delta^{18}\text{O}$  and SUS. This further confirmed climate shifted to more humid condition  
329 from MIS4 to early MIS3.

## 330 5.2 Carbon isotopes in land snail shells and vegetation changes

331 The carbon isotope of land snail shell is mainly related to carbon isotopes of dietary plants  
332 (Goodfriend and Ellis, 2002; Stott, 2002; Metref et al., 2003; Balakrishnan and Yapp, 2004).  
333 A previous study on modern land snails in China has shown that snail shell carbonate was  
334 enriched in  $^{13}\text{C}$  by  $14.2\text{‰}$  relative to snail body that has on isotopic difference from organic  
335 diet (Liu et al., 2006). At the same time,  $\text{C}_3$  and  $\text{C}_4$  plants have far different carbon isotope  
336 compositions, i.e., the average  $\delta^{13}\text{C}$  of  $\text{C}_3$  plant is  $-27.1 \pm 2.0\text{‰}$  whereas the average  $\delta^{13}\text{C}$  of  
337  $\text{C}_4$  plant is  $-13.1 \pm 1.2\text{‰}$  (Farquhar et al., 1989; O'Leary, 1998; Cerling, 1999). Therefore,  
338 the proportion of  $\text{C}_3$  to  $\text{C}_4$  plants in snail food can be estimated based on the shell-diet carbon

339 isotope fractionation and snail shell carbon isotope. Because there is a 1.3‰ decrease in the  
340  $\delta^{13}\text{C}$  of atmospheric  $\text{CO}_2$  since the industrial revolution due to the combustion of  $^{13}\text{C}$ -depleted  
341 fossil fuels, so-called Suess effect (Marino et al., 1992), the above two  $\delta^{13}\text{C}$  end-members for  
342  $\text{C}_3$  and  $\text{C}_4$  plants should be adjusted to -25.8‰ and -11.8‰, respectively, during the last two  
343 glacial-interglacial periods in our study.

344 The maximum  $\delta^{13}\text{C}$  of *C. pulveratrix* was -7.34‰ that occurred at MIS5. Considering  
345 shell-diet carbon isotope fractionation of +14.2‰, the converted dietary  $\delta^{13}\text{C}$  was -21.5‰  
346 and the inferred proportion of  $\text{C}_4$  plant was about 31%. The minimum  $\delta^{13}\text{C}$  of *C. pulveratrix*  
347 was -9.71‰ that showed at MIS7. The estimated relative  $\text{C}_4$  abundance was about 14%. In  
348 contrast, the most positive  $\delta^{13}\text{C}$  of *M. yantaiensis* was -3.05‰ that occurred at MIS3,  
349 corresponding to a relative  $\text{C}_4$  abundance of 61%. The most negative  $\delta^{13}\text{C}$  of *M. yantaiensis*  
350 was -5.03‰ that showed at MIS7, converting to 47% of  $\text{C}_4$  in the food. It can be seen that  
351 *M. yantaiensis* snails consumed more  $\text{C}_4$  plants than *C. pulveratrix*. We acknowledged that  
352 the proportion of  $\text{C}_4$  plants in snail's food was overestimated because land snails may also  
353 take in a small portion of soil carbonates that have more positive  $\delta^{13}\text{C}$  than  $\text{C}_3$  and  $\text{C}_4$  plants.  
354 However, this does not influence our assessing the relative changes in  $\text{C}_4$  abundances over  
355 different MIS stages.

356 To some extent, relative abundance of  $\text{C}_4$  plants can reflect the climate and seasonal  
357 changes. At seasonal level,  $\text{C}_4$  plants prefer to grow in the summer when there are more  
358 warmth and abundant precipitation whereas  $\text{C}_3$  plants grow in spring and autumn with  
359 relatively low temperature (Sage et al., 1999; Huang et al., 2012). At glacial/interglacial time-  
360 scale,  $\text{C}_4$  biomass tended to increase during warm/humid interglacial periods whereas  $\text{C}_3$   
361 biomass dominated during the cold/dry glacial periods (Liu et al., 2005; Yang et al., 2015). As  
362 shown in Figure 4, the  $\delta^{13}\text{C}$  of *C. pulveratrix* was mostly more negative than that of *M.*

363 *yantaiensis* at the same horizon. This may indicate that *C. pulveratrix* was more active in  
364 relatively cold/arid environments or seasons and accordingly ingested more C<sub>3</sub> plants. This is  
365 consistent with the phenomenon observed by Huang et al. (2012).

366 In general, the  $\delta^{13}\text{C}$  curve of *C. pulveratrix* has a positive correlation with the SUS curve  
367 and a negative correlation with the  $\delta^{18}\text{O}$  of *C. pulveratrix*. This indicates a linkage of C<sub>3</sub>/C<sub>4</sub>  
368 abundance in dietary food of land snails to climate changes. Specifically, the  $\delta^{13}\text{C}$  values of  
369 *C. pulveratrix* snail shell during late MIS7 were slightly more positive than those during  
370 MIS6, and the  $\delta^{13}\text{C}$  of *C. pulveratrix* during MIS3 was more positive than MIS2 and MIS4 as  
371 well (Figure 3). Because the feeding habits of the same snail would not largely change, the  
372 above variation in C<sub>4</sub> abundance in the snail's food may reflect the changes of C<sub>4</sub> biomass in  
373 natural vegetation along with climate, i.e., relative abundance of C<sub>4</sub> plants increased during  
374 the warm/humid interglacial (or interstadial) periods. This is in accordance to the  
375 aforementioned conclusion reached by previous studies (Liu et al., 2005; Yang et al., 2015).

### 376 5.3 The relationship between snail numbers of two species and environment change

377 During late MIS7, the number of cold-aridiphilous *C. pulveratrix* snail was relatively lower  
378 than that of sub-humidiphilous *M. yantaiensis* and the land snail *M. yantaiensis* had reached a  
379 peak amount. At this time, Md became finer, SUS value increased, and the shell  $\delta^{18}\text{O}$  values  
380 of both *C. pulveratrix* and *M. yantaiensis* shifted to more negative. These multiple proxies  
381 uniformly suggested that the warm and humid climate prevailed, which was suitable to the  
382 growth of sub-humidiphilous *M. yantaiensis*. In addition, a large number of stone artifacts  
383 were found at the depth of 11-13 m (MIS7) in the Beiyao section (Du and Liu, 2014),  
384 indicating strong human activities. The inferred warm/humid climatic condition was  
385 conducive to the intensified prehistoric human activities.

386 After entering MIS6, the number of cold-aridiphilous species increased and reached the

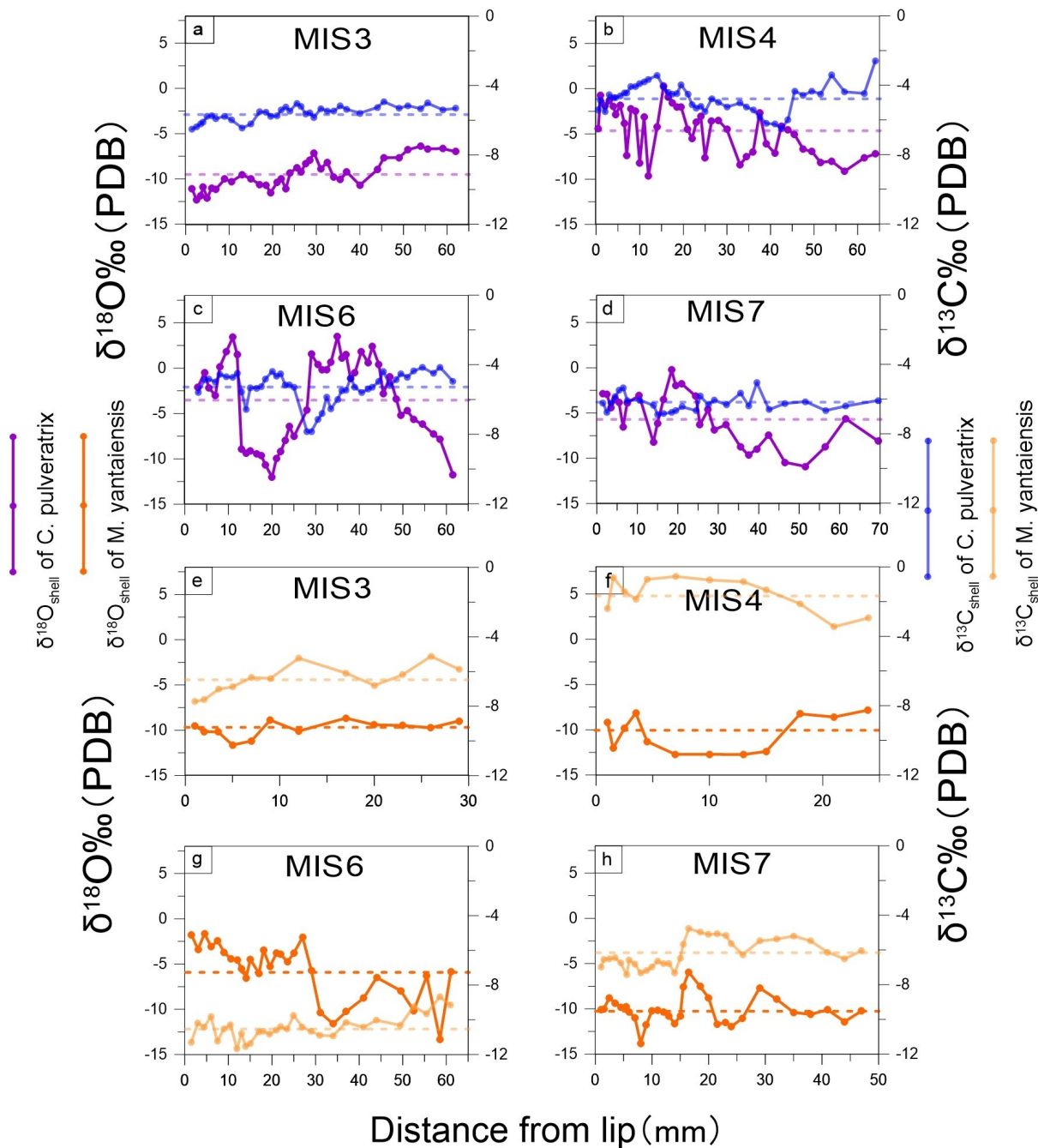
387 peak of the whole profile at 9.7 m whereas the sub-humidiphilous species almost  
388 disappeared, which implied the climate became much colder and drier than the previous  
389 stage. In the meantime, the  $\delta^{18}\text{O}$  of *C. pulveratrix* shifted to more positive value, i.e., up to -  
390 5.3‰, reflecting less monsoonal rainfall as well.

391 During most MIS5, land snail fossils were not preserved due to the influence of strong  
392 pedogenesis and there were only a few sub-humidiphilous snails at the depth of 6.5-7 m. At  
393 the end of MIS5, a small number of cold-aridiphilous species began to appear, indicating that  
394 the climate started to be relatively cold and dry, in accordance to the Md and SUS records.

395 To MIS4 stage, the number of cold-aridiphilous species significantly increased, reaching a  
396 maximum of 58, while sub-humidiphilous species rarely existed and even disappeared. The  
397 cold/dry climate as seen from the  $\delta^{18}\text{O}$  of *C. pulveratrix*, Md and SUS accounted for the  
398 flourish of the cold-aridiphilous *C. pulveratrix*.

399 During MIS3, the numbers of *C. pulveratrix* and *M. yantaiensis* showed alternative  
400 increases, further testifying variable climatic conditions. It also indicated that the climate was  
401 of moderate conditions so that both cold-aridiphilous and sub-humidiphilous species co-  
402 existed. At the early MIS3 stage, the number of *C. pulveratrix* decreased when *M. yantaiensis*  
403 reached its peak abundance. In contrast, both the numbers of *C. pulveratrix* and *M.*  
404 *yantaiensis* largely reduced at the middle MIS3. To the late MIS3, *M. yantaiensis* went further  
405 reduced but the number of *C. pulveratrix* increased. This assemblage change indicated that  
406 the climate was warmer and more humid at the early MIS3 than at late MIS3. A faunal  
407 assemblage study of land snails in central Chinese Loess Plateau also suggested that the  
408 temperature and humidity were higher during the early MIS3 (Chen and Wu, 2008).  
409 However, the  $\delta^{18}\text{O}$  of *C. pulveratrix* was highly variable during the early MIS3 and was not  
410 as more negative as that during the late MIS3 (Figure 3). This reflected a variable summer

411 monsoon and an overall less rainfall during the early MIS3.



412

413 **Figure 5.** Intra-shell variations of  $\delta^{18}\text{O}$  and  $\delta^{13}\text{C}$  for the two species at various MIS stages.

414

415 5.4 Intra-shell variation of stable isotopes and climate seasonality

416 In this study, intra-shell stable isotope analyses were performed on both *C. pulveratrix* and  
417 *M. yantaiensis* snails at MIS3, MIS4, MIS6, and MIS7, respectively. The measured *C.*  
418 *pulveratrix* and *M. yantaiensis* snails were chosen from the same layer (10 cm) in each MIS  
419 stage. During MIS3, the  $\delta^{18}\text{O}$  of *C. pulveratrix* and *M. yantaiensis* were among the most  
420 negative values of the four MIS stages, with averaged  $\delta^{18}\text{O}$  of -9.5‰ and -9.8‰,  
421 respectively. Moreover, the intra-shell variations in  $\delta^{18}\text{O}$  of the two snails were relatively  
422 small. For example, the  $\delta^{18}\text{O}$  of *C. pulveratrix* showed a variation magnitude of 5.9‰  
423 whereas  $\delta^{18}\text{O}$  of *M. yantaiensis* only changed by 2.9‰ (Figure 5a, e). This suggested a weak  
424 seasonality during the warm/humid MIS3 stage. Padgett et al. (2019) also observed a steady  
425 trend of  $\delta^{18}\text{O}$  in land snail shell in warm and humid climate. In contrast, the magnitudes of  
426 intra-shell  $\delta^{18}\text{O}$  variations for *C. pulveratrix* and *M. yantaiensis* showed large increases, i.e.,  
427 up to 10‰ and 4.9‰, respectively.

428 During MIS6, the average  $\delta^{18}\text{O}$  values of *C. pulveratrix* and *M. yantaiensis* became more  
429 positive and were around -3.6‰ and -5.7‰, respectively (Figure 5c, g). Meanwhile, the  
430 intra-shell  $\delta^{18}\text{O}$  of the two species exhibited largest variations during MIS6, i.e., a magnitude  
431 of 15.5‰ for *C. pulveratrix* and a magnitude of 12.1‰ for *M. yantaiensis*. These  
432 magnitudes were respectively 2.6 and 4 times of those for the same species during MIS3. It  
433 revealed extreme seasonal contrast during the cold/dry MIS6. It is worthy of mentioning that  
434 the intra-shell  $\delta^{18}\text{O}$  curve of *C. pulveratrix* displayed regular seasonal changes during MIS6  
435 (Figure 5c). Judging from the sinusoidal cycles, the *C. pulveratrix* snail may have a life span  
436 of about two years. The snail possibly started to grow from the summer of the first year to the  
437 autumn of the second year. The highest  $\delta^{18}\text{O}$  values recorded in the shell growing in the  
438 spring and autumn seasons attained to ca +2‰ and the lowest  $\delta^{18}\text{O}$  recorded in the shell

439 segments in summer was about -12‰. The large seasonal contrast was unlikely only  
440 attributed to temperature changes, which would be 56 °C offset if calculating by the  
441 carbonate oxygen isotope-temperature coefficient of 1‰ per 4 °C. Obviously, seasonal  
442 changes of rainfall largely contributed to the above fluctuation of  $\delta^{18}\text{O}$  of *C. pulveratrix*, that  
443 is, the negative values in shell  $\delta^{18}\text{O}$  being caused by rainfall amount effect in summer. An  
444 intra-shell  $\delta^{18}\text{O}$  study for the land snail collected from Ethiopia also revealed significant  
445 contribution of rainfall to the shape and amplitude of shell  $\delta^{18}\text{O}$  cycles (Leng et al., 1998).  
446 Except for the shell lip part, the  $\delta^{13}\text{C}$  of *C. pulveratrix* showed an overall opposite  
447 relationship with the shell  $\delta^{18}\text{O}$  (Figure 5c). When the  $\delta^{18}\text{O}$  was more negative in summer,  
448 the  $\delta^{13}\text{C}$  became more positive, implying the snail consumed increased amount of  $\text{C}_4$  plants in  
449 this season. In spring and autumn (at 30-45 mm from shell lip), more  $\text{C}_3$  plants were ingested  
450 by the snail. This seasonal change of  $\text{C}_3/\text{C}_4$  proportion in snail's food diet is consistent with  
451 the seasonal distribution of  $\text{C}_3$  and  $\text{C}_4$  plants in natural vegetation (Sage et al., 1999).

452 During MIS7, two individual shells for intra-shell isotope study were taken from the depth  
453 of 11.8 m, which happened to be within the period of strong prehistoric human activities (Du  
454 and Liu, 2014). Based on the previous discussions on  $\delta^{18}\text{O}$  of *C. pulveratrix* and *M.*  
455 *yantaiensis*, the climate was generally warm and humid during this time. The intra-shell  $\delta^{18}\text{O}$   
456 variations for *C. pulveratrix* and *M. yantaiensis* were at amplitudes of 10.7‰ and 10.9‰,  
457 respectively. The variations were smaller than those during MIS6. This overall small seasonal  
458 contrast was conducive to regional spread of human activity.

459 In summary, the average amplitude of intra-shell  $\delta^{18}\text{O}$  variations for *C. pulveratrix* was  
460 about 8.4‰ during the interglacial periods (i.e., MIS3 and MIS7), whereas it was 12.75‰  
461 during the glacial periods (i.e., MIS4 and MIS6). In the same manor, the intra-shell  $\delta^{18}\text{O}$  of

462 *M. yantaiensis* varied by 10.8‰ and 16.5‰, respectively, during the interglacial and glacial  
463 periods. Regardless of which species, the changing amplitude was 1.5 times larger during the  
464 glacial periods. Therefore, if the intra-shell variation of  $\delta^{18}\text{O}$  can be used to quantify the  
465 seasonal changes, the climatic seasonality during glacial periods would be about 1.5 times  
466 stronger than that during interglacial periods.

467 To explore the stable isotope differences among individual shells of each snail species from  
468 the same sampling horizon (10 cm layer), we analyzed  $\delta^{13}\text{C}$  and  $\delta^{18}\text{O}$  on *C. pulveratrix* from  
469 7 layers and *M. yantaiensis* from 3 layers. The carbon and oxygen isotope data were shown in  
470 Table 3. Firstly, within the same MIS (i.e., MIS3 or MIS7), the  $\delta^{18}\text{O}$  of sub-humidiphilous  
471 species (*M. yantaiensis*) showed little change, whereas the  $\delta^{18}\text{O}$  of cold-aridiphilous species  
472 (*C. pulveratrix*) distributed much discretely. This may indicate that sub-humidiphilous  
473 species have a more strict requirement on climate conditions, i.e., only grow during the  
474 period of abundant rainfall, while cold-aridiphilous species had strong adaptability and can  
475 survive under large range of climate conditions. Secondly, for the cold-aridiphilous species,  
476 the shell  $\delta^{18}\text{O}$  changes during the even-numbered MIS (i.e., MIS2, MIS4, and MIS6) were  
477 larger than those during the odd-numbered MIS (i.e., MIS3 and MIS7). Since the snail shells  
478 collected each sampling layer may not strictly come from the same time year, the above  
479 phenomenon may indicate that the climates within the time-span of each sampling layer  
480 during glacial periods (even-numbered MIS) were very unstable, whereas the climates during  
481 interglacial periods (odd-numbered MIS) had relatively stable and uniform conditions within  
482 the time period of each sampling layer. Previous studies have shown that climate during the  
483 last glacial period was quite unstable, with climate oscillations at centennial to millennium  
484 scales (Ren et al., 1996; Ding et al., 1998). This is in accordance to the large intra-species  
485 variation of shell  $\delta^{18}\text{O}$  in each sampling layer.

486

487 **Table 3** Statistics for intra-species  $\delta^{18}\text{O}$  and  $\delta^{13}\text{C}$  variations of two species at various MIS

488 stages.

| Species               | Depth<br>(m) | MI<br>S | Shell n<br>umber | $\delta^{18}\text{O}$<br>S.D. | $\delta^{18}\text{O}$<br>Max<br>(VPD<br>B) | $\delta^{18}\text{O}$<br>Min<br>(VPDB) | $\delta^{13}\text{C}$<br>S.D. | $\delta^{13}\text{C}$<br>Max<br>(VPDB) | $\delta^{13}\text{C}$<br>Min<br>(VPDB) |
|-----------------------|--------------|---------|------------------|-------------------------------|--------------------------------------------|----------------------------------------|-------------------------------|----------------------------------------|----------------------------------------|
| <i>C. pulveratrix</i> | 0.60         | 2       | 10               | 2.85                          | 1.34                                       | -7.65                                  | 0.99                          | -1.09                                  | -4.54                                  |
| <i>C. pulveratrix</i> | 1.80         | 3       | 10               | 2.47                          | -2.51                                      | -10.02                                 | 0.74                          | -3.68                                  | -5.83                                  |
| <i>C. pulveratrix</i> | 3.60         | 3       | 3                | 1.84                          | -5.93                                      | -9.33                                  | 1.52                          | -2.22                                  | -5.27                                  |
| <i>C. pulveratrix</i> | 4.6          | 3       | 10               | 2.11                          | -2.69                                      | -9.13                                  | 1.42                          | -2.62                                  | -7.06                                  |
| <i>C. pulveratrix</i> | 6.60         | 4       | 10               | 2.56                          | 1.10                                       | -6.71                                  | 0.83                          | -4.96                                  | -7.63                                  |
| <i>C. pulveratrix</i> | 9.10         | 6       | 10               | 1.98                          | -1.77                                      | -7.18                                  | 1.27                          | -1.22                                  | -5.88                                  |
| <i>C. pulveratrix</i> | 11.70        | 7       | 7                | 2.02                          | -5.32                                      | -10.55                                 | 2.34                          | 0.20                                   | -6.29                                  |
| <i>M. yantaiensis</i> | 3.60         | 3       | 5                | 1.26                          | -8.08                                      | -10.90                                 | 1.65                          | -1.93                                  | -6.31                                  |
| <i>M. yantaiensis</i> | 4.60         | 3       | 10               | 1.18                          | -5.60                                      | -8.92                                  | 2.20                          | 1.18                                   | -5.78                                  |
| <i>M. yantaiensis</i> | 11.70        | 7       | 10               | 1.13                          | -7.53                                      | -11.38                                 | 0.62                          | -2.70                                  | -4.80                                  |

489

490 **6 Conclusion**

491 In this study, we systematically analyzed stable carbon and oxygen isotopes on cold-  
492 aridiphilous *C. pulveratrix* and sub-humidiphilous *M. yantaiensis* snail shell fossils from the  
493 Beiyao loess-paleosol section in southeastern Chinese Loess Plateau. Stable isotopes were  
494 measured on both the mixed multiple shells and the single shell along the growth band. The  
495 obtained  $\delta^{13}\text{C}$  and  $\delta^{18}\text{O}$  data were compared with Md and SUS from the same profile and  
496 deep-ocean  $\delta^{18}\text{O}$  curve to verify the reliability of snail shell stable isotopes for paleoclimate  
497 reconstruction. We reached the following conclusions:

498 1.  $\delta^{18}\text{O}$  of snail shells in strata can be used to indicate the intensity of summer monsoon

499 rainfall. During MIS7 and MIS3 stages, the shell  $\delta^{18}\text{O}$  was more negative, indicating strong  
500 monsoonal rainfall, which showed a good correlation to Md, SUS, and deep-sea  $\delta^{18}\text{O}$  curve.  
501 Meanwhile, the shell  $\delta^{13}\text{C}$  can reflect the proportion of  $\text{C}_4$  plants in snail's food and  
502 ultimately trace the relative abundance of  $\text{C}_4$  plants in contemporary vegetation. The results  
503 showed that the relative abundance of  $\text{C}_4$  plants increased during the warm/humid MIS7 and  
504 MIS3.

505 2. The stable isotopes of *C. pulveratrix* and *M. yantaiensis* from the same horizon were  
506 largely different, reflecting differences in their eco-physiological habits. The  $\delta^{18}\text{O}$  of *M.*  
507 *yantaiensis* was significantly lower than that of *C. pulveratrix*, indicating that *M. yantaiensis*  
508 lived in warmer and more humid conditions than *C. pulveratrix*. The  $\delta^{13}\text{C}$  of *M. yantaiensis*  
509 was mostly higher than that of *C. pulveratrix*, suggesting that *M. yantaiensis* ingested more  
510  $\text{C}_4$  plants than *C. pulveratrix*.

511 3. Intra-shell  $\delta^{18}\text{O}$  variations revealed that there was a significant difference in the climatic  
512 seasonality between glacial and interglacial periods. During the glacial periods (even-  
513 numbered MIS), the seasonal contrast was large, whereas the seasonal contrast was small  
514 during the interglacial periods (odd-numbered MIS). Stable isotope analyses of multiple  
515 shells of the same snail species within each sampling layer showed that intra-species isotope  
516 data were largely scattered during the glacial periods, indicative of highly unstable climates  
517 change at sub-millennial scale, whereas intra-species isotopic difference was relatively small  
518 during the interglacial periods, suggestive of a steady and uniform climatic condition within  
519 millennium.

520 4. During MIS3 and MIS7, there were evidences of human activities around the Beiyao site,  
521 but the corresponding climate background remained unclear. By analyzing whole-shell and  
522 intra-shell  $\delta^{18}\text{O}$  and faunal assemblage of the two species snails, we concluded that the

523 climates were relatively warm and humid with a weak seasonality. This stable climatic  
524 condition was conducive to the regional expansion of prehistoric human activities.

#### 525 **Acknowledgement:**

526 This work was supported by National Natural Science Foundation of China (Grant No.  
527 41572163), the National Key R&D Program of China (Grant No. 2017YFA0603400), and  
528 National Natural Science Foundation of China (Grant No. 41872080). Thanks to Yue Jiaojiao  
529 for assistance in taking photo of the snails shells. Data for producing Figures 3–5 are  
530 available from the data share website and the DOI is 10.6084/m9.figshare.12190485.

531

#### 532 **References**

- 533 Balakrishnan, M., & Yapp, C. J. (2004). Flux balance models for the oxygen and carbon  
534 isotope compositions of land snail shells. *Geochimica et Cosmochimica Acta*, 68(9), 2007-  
535 2024. <https://doi.org/10.1016/j.gca.2003.10.027>
- 536 Bao, R., Sheng, X., Lu, H., Li, C., Luo, L., Shen, H., et al. (2019). Stable carbon and oxygen  
537 isotopic composition of modern land snails along a precipitation gradient in the mid-latitude  
538 East Asian monsoon region of China. *Palaeogeography, Palaeoclimatology, Palaeoecology*  
539 553, 109236. <https://doi.org/10.1016/j.palaeo.2019.109236>
- 540 Bao, R., Sheng, X., Teng, H. H., & Ji, J. (2018). Reliability of shell carbon isotope  
541 composition of different land snail species as a climate proxy: A case study in the monsoon  
542 region of China. *Geochimica et Cosmochimica Acta*, 228, 42-61.  
543 <https://doi.org/10.1016/j.gca.2018.02.022>
- 544 Cerling, T. E. (1999). Paleorecords of C4 plants and ecosystems. *C4 plant biology*, 445-469.
- 545 Chen, D. N., & Zhang, G. Q. (2004). Fauna Sinica, Invertebrata, Mollusca, Gastripoda,

546 Stylommatophora Bradybaenidae [in Chinese], **37**, pp. 250-399, Science, Beijing.

547 Chen, X. Y., & Wu, N. Q. (2008). Relatively warm-humid climate recorded by mollusk  
548 species in the Chinese Loess Plateau during MIS 3 and its possible forcing mechanism.  
549 *Quaternary Sciences*, *28*, 154-161.

550 Colonese, A. C., Zanchetta, G., Dotsika, E., Drysdale, R. N., Fallick, A. E., Grifoni  
551 Cremonesi, R., et al. (2010). Early-middle Holocene land snail shell stable isotope record  
552 from Grotta di Latronico 3 (southern Italy). *Journal of Quaternary Science*, *25*(8), 1347-  
553 1359. <https://doi.org/10.1002/jqs.1429>

554 Ding, Z. L., Rutter, N. W., Liu, T. S., Sun, J. M., Ren, J. Z., Rokosh, D., et al. (1998).  
555 Correlation of Dansgaard-Oeschger cycles between Greenland ice and Chinese loess.  
556 *Paleoclimates*, *4*, 281-291.

557 Du, S. S., Yang, L. R., Liu, F. L., & Ding, Z. L. (2011). Re-examination of the age of the  
558 Beiyao site, Luoyang City. *Quaternary Sciences*, *31*, 16-21.

559 Du, S. S., & Liu, F. L. (2014). Loessic palaeolith discovery at the Beiyao site, Luoyang, and  
560 its implications for understanding the origin of modern humans in Northern China.  
561 *Quaternary International*, *349*, 308-315. <https://doi.org/10.1016/j.quaint.2014.05.037>

562 Farquhar, G. D., Ehleringer, J. R., & Hubick, K. T. (1989). Carbon isotope discrimination and  
563 photosynthesis. *Annual review of plant biology*, *40*(1), 503-537.  
564 <https://doi.org/10.1146/annurev-food-032519-051632>

565 Gittenberger, E., & Goodfriend, G. A. (1993). Land snails from the last glacial maximum on  
566 Andikithira, southern Greece and their palaeoclimatic implications. *Journal of Quaternary  
567 Science*, *8*(2), 109-116. <https://doi.org/10.1002/jqs.3390080203>

568 Goodfriend, G. A. (1992). The use of land snail shells in paleoenvironmental reconstruction.  
569 *Quaternary Science Reviews*, *11*(6), 665-685. [https://doi.org/10.1016/0277-3791\(92\)90076-](https://doi.org/10.1016/0277-3791(92)90076-)

570 K

571 Goodfriend, G. A., & Ellis, G. L. (2002). Stable carbon and oxygen isotopic variations in  
572 modern *Rabdotus* land snail shells in the southern Great Plains, USA, and their relation to  
573 environment. *Geochimica et Cosmochimica Acta*, 66(11), 1987-2002.  
574 [https://doi.org/10.1016/S0016-7037\(02\)00824-4](https://doi.org/10.1016/S0016-7037(02)00824-4)

575 Gu, Z. Y., Liu, Z. X., Xu, B., & Wu, N. Q. (2009). Stable carbon and oxygen isotopes in land  
576 snail carbonate shells from a last glacial loess sequence and their implications of  
577 environmental changes. *Quaternary Science*, 29, 13-22.

578 Huang, L. P., Wu, N. Q., Gu, Z. Y., & Chen, X. Y. (2012). Variability of snail growing season  
579 at the Chinese Loess Plateau during the last 75 ka. *Chinese science bulletin*, 57(9), 1036-  
580 1045.

581 Kukla, G., An, Z. S., Melice, J. L., Gavin, J., & Xiao, J. L. (1990). Magnetic susceptibility  
582 record of Chinese loess. *Earth and Environmental Science Transactions of the Royal Society  
583 of Edinburgh*, 81(4), 263-288. <https://doi.org/10.1017/S0263593300020794>

584 Leng, M. J., Heaton, T. H., Lamb, H. F., & Naggs, F. (1998). Carbon and oxygen isotope  
585 variations within the shell of an African land snail (*Limicolaria kambeul chudeau* Germain):  
586 a high-resolution record of climate seasonality? *The Holocene*, 8(4), 407-412.  
587 <https://doi.org/10.1191/095968398669296159>

588 Liu, W. G., Huang, Y. S., An, Z. S., Clemens, S. C., Li, L., Prell, W. L., & Ning, Y. F.  
589 (2005). Summer monsoon intensity controls C4/C3 plant abundance during the last 35 ka in  
590 the Chinese Loess Plateau: carbon isotope evidence from bulk organic matter and individual  
591 leaf waxes. *Palaeogeography, Palaeoclimatology, Palaeoecology*, 220(3-4), 243-254.  
592 <https://doi.org/10.1016/j.palaeo.2005.01.001>

593 Liu, Z. X., Gu, Z. Y., Bing, X., & Wu, N. Q. (2006). Monsoon precipitation effect on oxygen

594 isotope composition of land snail shell carbonate from Chinese loess plateau. *Quaternary*  
595 *Sciences* 26, (4), 643-648.

596 Liu, Z. X., Gu, Z. Y., Wu, N. Q., & Xu, B. (2007). Diet control on carbon isotopic  
597 composition of land snail shell carbonate. *Chinese Science Bulletin*, 52(3), 388-394.

598 O'Leary, M. H. (1988). Carbon isotopes in photosynthesis. *Bioscience*, 38(5), 328-336.

599 Marino, B. D., McElroy, M. B., Salawitch, R. J., & Spaulding, W. G. (1992). Glacial-to-  
600 interglacial variations in the carbon isotopic composition of atmospheric CO<sub>2</sub>. *Nature*,  
601 357(6378), 461-466.

602 Martinson, D. G., Pisias, N. G., Hays, J. D., Imbrie, J., Moore, T. C., & Shackleton, N. J.  
603 (1987). Age dating and the orbital theory of the ice ages: Development of a high-resolution  
604 0 to 300,000-year chronostratigraphy 1. *Quaternary research*, 27(1), 1-29.  
605 [https://doi.org/10.1016/0033-5894\(87\)90046-9](https://doi.org/10.1016/0033-5894(87)90046-9)

606 Metref, S., Rousseau, D. D., Bentaleb, I., Labonne, M., & Vianey-Liaud, M. (2003). Study of  
607 the diet effect on  $\delta^{13}\text{C}$  of shell carbonate of the land snail *Helix aspersa* in experimental  
608 conditions. *Earth and Planetary Science Letters*, 211(3-4), 381-393. [https://doi.org/10.1016/](https://doi.org/10.1016/S0012-821X(03)00224-3)  
609 [S0012-821X\(03\)00224-3](https://doi.org/10.1016/S0012-821X(03)00224-3)

610 Milano, S., Demeter, F., Hublin, J. J., Düringer, P., Patole-Edoumba, E., Ponche, J. L., et al.  
611 (2018). Environmental conditions framing the first evidence of modern humans at Tam Pà  
612 Ling, Laos: A stable isotope record from terrestrial gastropod carbonates. *Palaeogeography,*  
613 *Palaeoclimatology,* *Palaeoecology*, 511, 352-363.  
614 <https://doi.org/10.1016/j.palaeo.2018.08.020>

615 Nevo, E., Bar-El, C., & Bar, Z. (1983). Genetic diversity, climatic selection and speciation of  
616 *Sphincterochila* landsnails in Israel. *Biological Journal of the Linnean Society*, 19(4), 339-  
617 373.

618 Padgett, A., Yanes, Y., Lubell, D., & Faber, M. L. (2019). Holocene cultural and climate shifts  
619 in NW Africa as inferred from stable isotopes of archeological land snail shells. *The*  
620 *Holocene*, 29(6), 1078-1093. <https://doi.org/10.1177/0959683619831424>

621 Prendergast, A. L., Stevens, R. E., Hill, E. A., Hunt, C., O'Connell, T. C., & Barker, G. W.  
622 (2017). Carbon isotope signatures from land snail shells: Implications for palaeovegetation  
623 reconstruction in the eastern Mediterranean. *Quaternary International*, 432, 48-57.  
624 <https://doi.org/10.1016/j.quaint.2014.12.053>

625 Prendergast, A. L., Stevens, R. E., O'Connell, T. C., Hill, E. A., Hunt, C. O., & Barker, G. W.  
626 (2016). A late Pleistocene refugium in Mediterranean North Africa? Palaeoenvironmental  
627 reconstruction from stable isotope analyses of land snail shells (Haua Fteah, Libya).  
628 *Quaternary Science Reviews*, 139, 94-109. <https://doi.org/10.1016/j.quascirev.2016.02.014>

629 Puisségur, J. J. (1976). *Mollusques continentaux quaternaires de Bourgogne: significations*  
630 *stratigraphiques et climatiques, rapports avec d'autres faunes boréales de France* (No. 3).  
631 Diffusion, Doin.

632 Rangarajan, R., Ghosh, P., & Naggs, F. (2013). Seasonal variability of rainfall recorded in  
633 growth bands of the Giant African Land Snail *Lissachatina fulica* (Bowdich) from India.  
634 *Chemical Geology*, 357, 223-230. <https://doi.org/10.1016/j.chemgeo.2013.08.015>

635 Ren, J. Z., Ding, Z. L., Liu, D. S., Sun J. M., Zhou, Q. X. 1996. Climatic changes on  
636 millennial time scales- evidence from a high-resolution loess record. *Science in China*  
637 *(Series D)*, 39, 449-459.

638 Sage, R. F., Wedin, D. A., & Li, M. (1999). The biogeography of C4 photosynthesis: patterns  
639 and controlling factors. *C4 plant biology*, 313-373.

640 Stott, L. D. (2002). The influence of diet on the  $\delta^{13}\text{C}$  of shell carbon in the pulmonate snail  
641 *Helix aspersa*. *Earth and Planetary Science Letters*, 195(3-4), 249-259.

642 [https://doi.org/10.1016/S0012-821X\(01\)00585-4](https://doi.org/10.1016/S0012-821X(01)00585-4)

643 Tang, Z. H., Du, S. S., & Liu, F. L. (2017). Late Pleistocene changes in vegetation and the  
644 associated human activity at Beiyao Site, Central China. *Review of Palaeobotany and*  
645 *Palynology*, 244, 107-112. <https://doi.org/10.1016/j.revpalbo.2017.04.002>

646 Wang, X., Cui, L. L., Zhai, J. X., & Ding, Z. L. (2016). Stable and clumped isotopes in shell  
647 carbonates of land snails *Cathaica* sp. and *Bradybaena* sp. in north China and implications  
648 for ecophysiological characteristics and paleoclimate studies. *Geochemistry, Geophysics,*  
649 *Geosystems*, 17(1), 219-231. <https://doi.org/10.1002/2015GC006182>

650 Wang, X., Zhai, J. X., Cui, L. L., Zhang, S. H., & Ding, Z. (2019). Stable carbon and oxygen  
651 isotopes in shell carbonates of modern land snails in China and their relation to environment  
652 variables. *Journal of Geophysical Research: Biogeosciences*, 124(11), 3356-3376.  
653 <https://doi.org/10.1029/2019JG005255>

654 Wu, N. Q., Rousseau, D. D., & Liu, T. S. (1996). Land mollusk records from the Luochuan  
655 loess sequence and their paleoenvironmental significance. *Science in China (Series D)*, 39,  
656 494-502.

657 Wu, N. Q., Liu, X. P., Gu, Z. Y., & Pei, Y. P. (2002). Rapid climate variability recorded by  
658 mollusk species on the loess plateau during the last glacial maximum. *Quaternary Sciences*,  
659 22(3), 283-291

660 Wu, N. Q., & Li, F. J. (2008). Terrestrial mollusk fossils from Chinese loess sequence and  
661 their paleoenvironmental significance. *Quaternary Sciences*, 28(5), 831-840

662 Wu, N. Q., Li, F. J., & Rousseau, D. D. (2018). Terrestrial mollusk records from Chinese  
663 loess sequences and changes in the East Asian monsoonal environment. *Journal of Asian*  
664 *Earth Sciences*, 155, 35-48. <https://doi.org/10.1016/j.jseaes.2017.11.003>

665 Wu Y, (2011). The Study of East Asian Monsoon Variations In the Last Two Glaciations:

666 Evidence From Terrestrial Mollusk Record In Beiyao. (master's thesis), Beijing Normal  
667 University, pp.1-30.

668 Xu, B., Gu, Z. Y., Han, J. T., Liu, Z. X., Pei, Y. P., Lu, Y. W., et al. (2010). Radiocarbon and  
669 stable carbon isotope analyses of land snails from the Chinese loess plateau: environmental  
670 and chronological implications. *Radiocarbon*, 52(1), 149-156.  
671 <https://doi.org/10.1017/S0033822200045094>

672 Yanes, Y., & Fernández-Lopez-de-Pablo, J. (2017). Calibration of the stable isotope  
673 composition and body size of the arid-dwelling land snail *Sphincterochila candidissima*, a  
674 climatic archive abundant in Mediterranean archaeological deposits. *The Holocene*, 27(6),  
675 890-899. <https://doi.org/10.1177/0959683616675943>

676 Yang, S. L., Ding, Z. L., Li, Y. Y., Wang, X., Jiang, W. Y., & Huang, X. F. (2015). Warming-  
677 induced northwestward migration of the East Asian monsoon rain belt from the Last Glacial  
678 Maximum to the mid-Holocene. *Proceedings of the National Academy of Sciences*, 112(43),  
679 13178-13183. <https://doi.org/10.1073/pnas.1504688112>

680 Zaarur, S., Olack, G., & Affek, H. P. (2011). Paleo-environmental implication of clumped  
681 isotopes in land snail shells. *Geochimica et Cosmochimica Acta*, 75(22), 6859-6869. [https://](https://doi.org/10.1016/j.gca.2011.08.044)  
682 [doi.org/10.1016/j.gca.2011.08.044](https://doi.org/10.1016/j.gca.2011.08.044)